

# Ordinary Hall effect in MBE-grown MnAs films grown on GaAs(001) and GaAs(111)B

K.-J. Friedland,\* M. Kästner, and L. Däweritz

*Paul-Drude-Institut für Festkörperelektronik, Hausvogteiplatz 5–7, 10117 Berlin, Germany*

(Received 16 September 2002; published 4 March 2003)

We study the low-temperature magnetoresistance in thin, high-quality MnAs layers on GaAs. The ordinary Hall effect depends sensitively on the epitaxial orientation of the MnAs layer. We use a simplified model to interpret the sign reversal of the Hall resistivity as a function of the magnetic field together with the large positive magnetoresistivity. For  $A_0$ -oriented MnAs films with the  $c$  axis oriented in the plane, we conclude that the low-temperature carrier transport is dominantly holelike at zero magnetic fields, which then undergoes a transition to mixed holelike and electronlike conductivity at high magnetic fields. MnAs films with an out-of-plane oriented  $c$  axis show a mixed carrier conductivity already at zero magnetic fields. The possible influence of interface/surface scattering in high-quality MnAs layers on the transfer of holelike to electronlike conductivity is discussed.

DOI: 10.1103/PhysRevB.67.113301

PACS number(s): 73.25.+i, 73.50.-h, 75.50.Cc

Hybrid structures consisting of ferromagnetic metal layers on semiconductors have recently attracted much attention due to their potential in spintronics. One important effort is to realize spin injection from metals into semiconductors<sup>1,2</sup> with the additional degree of freedom of manipulating spins in the semiconductor. The room-temperature ferromagnet MnAs can be epitaxially grown on GaAs and exhibits excellent structural and magnetic properties.<sup>3,4</sup> The knowledge of the carrier properties in the ferromagnet is of critical importance in order to utilize the hybrid structure. The detailed investigation of the magnetoresistivity and its temperature dependence allows us to characterize the carriers at the Fermi surface. A two-carrier transport with a transition between the electron- and hole-dominated transport regimes was suggested for MnAs films on GaAs,<sup>5</sup> which is, for example, of direct relevance for spin-injection experiments. This conclusion was drawn mainly because of the observed sign reversal of the Hall resistivity with increasing magnetic fields at low temperatures. At the same time, a sign reversal of the Hall resistivity was discussed as a transition phenomena from low fields to high fields, when different momentum orbits at the Fermi surface contribute to the conductivity, as it was shown for the Hall effect in Co (Ref. 6) and Fe.<sup>7</sup>

In order to investigate, if the complex structure of the Fermi surface comes into the play in experiments with high magnetic fields, we have studied the magnetotransport in MnAs films with different epitaxial orientations grown on semi-insulating GaAs(001) and GaAs(111)B. Our results show that the type of carrier transport depends on the epitaxial orientation. We will use a simple model to describe the magnetic-field dependence of the resistivity tensor by changing the contribution of electronlike and holelike conductivity with magnetic field.

The samples were grown using standard solid-source molecular-beam epitaxy on GaAs(001) and GaAs(111)B substrates. The surface reconstruction and crystallographic orientation were monitored by reflection high-energy electron diffraction. Ferromagnetic MnAs layers were grown on a 100 nm GaAs buffer layer at a substrate temperature of 250 °C. Different epitaxial orientations were obtained by growing MnAs on different template structures with different

As<sub>4</sub> coverage/reconstruction and by varying the ratio of the beam equivalent pressure (BEP) ratio of As<sub>4</sub> and Mn. The  $A_0$  orientation, where the crystallographic  $c$  axis lies in the film plane and is oriented along the GaAs  $[1\bar{1}0]$  direction, was obtained by growing on an As-rich GaAs(001)-(4×4) template<sup>3,8</sup> at a growth rate of 20–25 nm/h and a BEP ratio of 300. Another orientation, which we call  $A_1$  orientation, was obtained by growing on a GaAs(001)-(2×4) template at a growth rate of 140 nm/h and a BEP ratio of 10. In this case, the samples consist of domains with 29° out-of-plane orientations of the  $c$  axis, whose projection in the film plane is parallel to the GaAs  $[1\bar{1}0]$  direction as for the  $A_0$  orientation. The MnAs  $c$  axis, which is the crystallographic hard axis of magnetization,<sup>9</sup> determines the direction of the magnetic hard axis in the film, which is oriented along the GaAs  $[1\bar{1}0]$  direction for both orientations. In MnAs layers grown on a GaAs(111)B-(2×2) template at a growth rate of 20 nm/h and a BEP ratio of 120, the  $c$  axis is oriented perpendicular to the film plane.<sup>10</sup>

We will present experimental results for four different samples. The sample thicknesses and orientations are listed in Table I. The high quality of the layers is demonstrated by the resistance ratio  $\rho(300\text{ K})/\rho(1.2\text{ K})$ , which is 600 for the 180 nm thick sample  $S_1$ , 40 for the 20 nm thick samples  $S_2$  and  $S_3$ , and 60 for the 50 nm thick sample  $S_4$ . For the magnetoresistance measurements, we used rectangular specimens with current flowing either in the GaAs  $[1\bar{1}0]$  or GaAs  $[110]$  directions with Ohmic contacts in a conventional Hall geometry by bonding Au wires onto the layer at the sample boundary. We carefully aligned the Hall contacts along equal potential lines in zero magnetic field. However, because of the low Hall resistivity  $\rho_{xy}$  in comparison with the longitudinal resistivity  $\rho_{xx}$ , a significant crossover from  $\rho_{xx}$  to  $\rho_{xy}$  may occur. In this case, we corrected  $\rho_{xy}$  using the relation  $\rho_{xy}^{\text{corr}}(H) = \rho_{xy}(H) - \rho_{xy}(0)/\rho_{xx}(0) \times \rho_{xx}(H)$  and proved that  $\rho_{xy}^{\text{corr}}(H)$  is an odd function of the magnetic field  $H$ .

Because of the ferromagnetic properties of the layers,  $\rho_{xx}$  and  $\rho_{xy}$  depend on the magnetic field, the field orientation, and temperature. For in-plane magnetic fields, the magne-

TABLE I. The thickness  $d$ , the orientation, the carrier densities  $p$  and  $n$ , the inverse mobilities  $S^h$  and  $S^e$ , the scattering rate for the transition from holelike to electronlike orbits  $S^l$ , and the hole mean free path  $L^h$  obtained from the fit of the magnetoresistance data at  $T=0.3$  K. An asterisk indicates a value obtained at large magnetic fields.

Sample	$d$ (nm)	MnAs orientation	$p$ (per unit cell)	$n$ (per unit cell)	$S^h$ (V s/m <sup>2</sup> )	$S^e$ (V s/m <sup>2</sup> )	$S^l$ (V s/m <sup>2</sup> )	$L^h$ (nm)
S1	180	$A_0$	1.2 0.22*	0 0.08*	31	10	1.8	225
S2	20	$A_0$	1.2	0	400	91	29	18
S3	20	$A_1$	1.8	0.2	240	30	83	33
S4	50	$c \parallel n$	0.10	0.09	33	27	>100	90

toresistivity tensor is highly anisotropic and mainly determined by the hindered rotation of the magnetic moment. Here, we discuss only the ordinary Hall effect with the magnetic field perpendicular to the surface at low temperatures. At temperatures below 1 K, the longitudinal resistivity  $\rho_{xx}$  is low and, therefore, the anomalous Hall effect in the MnAs films becomes negligibly small. Additionally, in this case there is no significant anisotropy with current flowing in the GaAs  $[1\bar{1}0]$  or GaAs  $[110]$  directions. The low-temperature magnetoresistance  $\rho_{xy}$  [ $\rho_{xx}$ ] is shown in Figs. 1(a) and 1(b) [Figs. 1(c) and 1(d)] for the four samples as a function of the magnetic field. As already reported by Berry *et al.*,<sup>5</sup> the  $A_0$ -oriented MnAs films show a Hall resistivity with a positive slope at low magnetic fields. The slope changes to negative values at higher magnetic fields, and even the Hall resistivity becomes negative at the highest magnetic fields. At the same time, these samples exhibit a large positive magnetoresistivity of more than 420% at  $H=120$  kOe (sample S1 with the lowest resistivity). In contrast, the slope and the Hall-resistivity are already negative for the lowest magnetic field values in films with an out-of-plane oriented  $c$  axis. In addition, these films show a much smaller magnetoresistivity

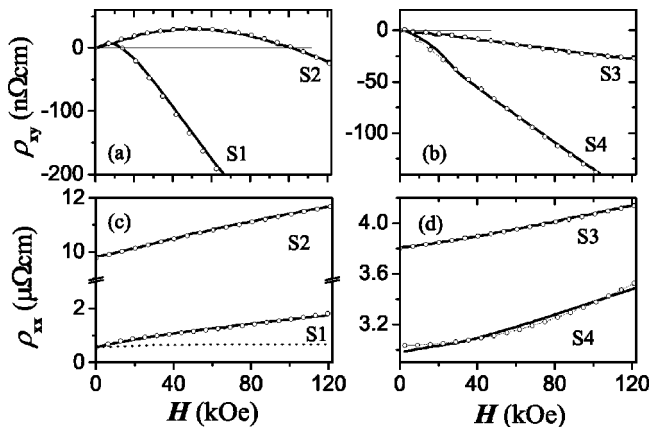


FIG. 1. Hall resistivities for samples (a) S1 and S2 with  $A_0$  orientation and (b) S3 and S4 with out-of-plane orientation of the  $c$  axis and the corresponding magnetoresistivities in (c) and (d) as a function of the magnetic field  $H$  at  $T=0.3$  K. Open circles represent the fit to our model with respect to the true field in the sample. The dotted line in (c) represents  $\rho_{xx}(H)$  calculated from the parameters for a fit of  $\rho_{xy}(H)$  in S1 with the simple two-band model.

with a maximum value of only 17%. Following the quantitative analysis of two-band magnetotransport in half-metallic chromium dioxide,<sup>11</sup> the nonlinear dependence and the sign reversal of the Hall resistance  $\rho_{xy}$  with increasing magnetic field was interpreted as a two-carrier transport, dominantly holes at high temperatures and dominantly electrons at low temperatures.<sup>5</sup> However, we will show that the simple model of two-carrier transport cannot account for the observed magnetotransport data in high-quality MnAs films. Moreover, we will show that a carrier-type transition appears at  $\omega_c \tau \cong 1$ , where  $\omega_c$  is the cyclotron frequency and  $\tau$  the scattering time.

The model for the classical two-carrier transport in the Hall geometry is based on the assumption that the components of the conductivity tensor  $\hat{\sigma}$  are additive in the conductivities for each carrier channel, in particular electrons ( $e$ ) and holes ( $h$ ):

$$\sigma_{ij} = \sigma_{ij}^h + \sigma_{ij}^e. \quad (1)$$

The indices  $i, j$  define the coordinates  $x, y$  in the plane perpendicular to the magnetic field direction. For spherical hole and electron Fermi surfaces,  $\sigma_{ij}^h$  and  $\sigma_{ij}^e$  have the form

$$\begin{aligned} \sigma_{yy}^l = \sigma_{xx}^l = \sigma_0^l \frac{1}{1 + (H/S^l)^2}, \\ \sigma_{xy}^l = -\sigma_{yx}^l = \pm \sigma_0^l \frac{(H/S^l)}{1 + (H/S^l)^2}, \end{aligned} \quad (2)$$

where  $l=h, e$  and  $\sigma_0^l = e \times n^l / S^l$ . The plus (minus) sign corresponds to the hole (electron) conductivity with the density  $n^h = p$  ( $n^e = n$ ). Within this model,  $S^l$  denotes inverse mobilities and  $H/S^l = \omega_c \tau$ . For asymmetric scattering in ferromagnetic metals,  $S^l$  becomes a tensor.<sup>12</sup> The resistivity tensor  $\hat{\rho}$  is obtained by inverting  $\hat{\sigma}$ . However, using this model, we could not find an adequately and simultaneously fit of the field-dependent Hall resistivity  $\rho_{xy}(H)$  together with the magnetoresistivity  $\rho_{xx}(H)$  for all four samples by varying the parameters  $n$ ,  $p$ ,  $S^e$ , and  $S^h$  even when taking into account anisotropic scattering at magnetic moments. As an example, we show in Figs. 1(a) and 1(b) a fit according to a procedure described in Ref. 11, which exhibits two major discrepancies. First, within the simple two-carrier transport

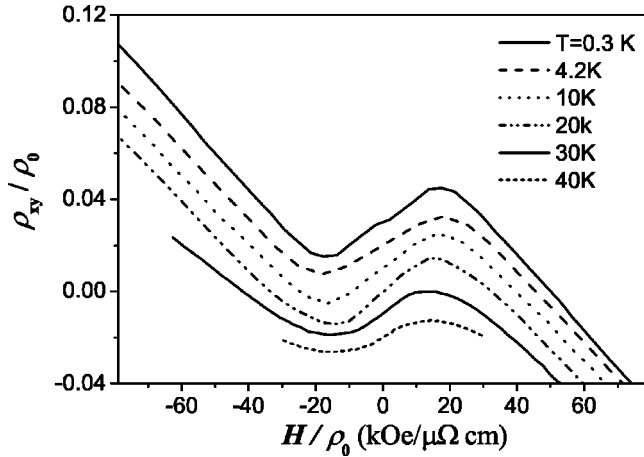


FIG. 2. Kohler plot of the Hall resistivities for sample *S1* at several temperatures as indicated. The traces are shifted by  $\rho_{xy}/\rho_0 = |0.01|$  at  $H=0$  for clarity.

model, the magnetoresistivity saturates at high fields,<sup>13</sup> which we do not observe in our films. Second, we obtain unrealistic mean free paths  $L^h$ , which are much larger than the film thicknesses, e.g.,  $1/S^h = 0.58 \text{ m}^2/\text{Vs}$  in the sample *S1*, which corresponds to  $L^h \approx 1 \text{ }\mu\text{m}$ . This would suggest that scattering at the interface/surface is negligible, which contradicts, however, our observation that the resistivity drastically increases with the reduction of the film thickness for similar growth conditions. For the sample *S1* with the lowest resistivity,  $\rho_{xx}(H)$  increases up to our highest magnetic fields without any sign of saturation. Earlier investigations of the magnetoresistivity relate this behavior to non-spherical Fermi surfaces in reciprocal space with open orbits.<sup>13</sup> However, a fit with open orbits was not successful for our experimental data. The nonlinearity or the sign reversal of  $\rho_{xy}(H)$  are discussed as a result of scattering<sup>6,7</sup> or magnetic breakdown<sup>14</sup> between different sheets of carriers at the Fermi surface under the condition  $\omega_c\tau \geq 1$ . To prove the low-field to high-field transition nature of the observed sign reversal of  $\rho_{xy}(H)$ , we show in Fig. 2 the data of the sample *S1* for different temperatures in a Kohler plot, where the ratio  $\rho_{xy}/\rho_0$  is plotted as a function of  $H/\rho_0$ .  $\rho_0$  is the zero-field resistivity, which changes drastically with temperature. Fortunately, a sufficiently large temperature interval from 0.3–40 K exists in this sample, where the anomalous Hall effect vanishes, but  $\rho_0$  changes from 0.4 to 2.5  $\mu\Omega \text{ cm}$ . Obviously, the change in the Hall conductivity occurs at the same  $H/\rho_0$  value, which is proportional to  $\omega_c\tau$ , rather than at the same field value  $H$  for different temperatures and layer thicknesses. We interpret this behavior as a strong indication that the low-field to the high-field transition in the Hall effect has its origin in the unique Fermi-surface topology. Band structure calculations for MnAs show the more complex topology of the Fermi surface.<sup>15–17</sup> Therefore, extended path-integral calculations are necessary in order to model the magnetoresistivity<sup>14</sup> as a function of the contributions of different momentum orbits, the temperature, and the magnetic field. Such calculations are far beyond the scope of this paper.

Nevertheless, we will present a simple model, which al-

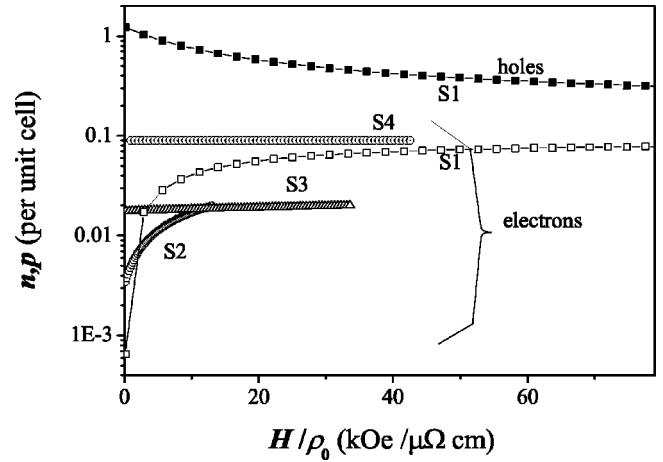


FIG. 3. Calculated carrier densities as a function of  $H/\rho_0$  at  $T = 0.3 \text{ K}$ .

lows to account for the change of the carrier transport type from holelike to electronlike by changing  $\omega_c\tau$ . We suppose that with increasing  $\omega_c\tau$  more momentum space becomes accessible, which may result in a change of the scattering process, such as intersheet scattering with Umklapp scattering<sup>14</sup> or an increase of electron orbits at the expense of holes.<sup>6</sup> To account for the different contributions of electrons and holes to the conductivity, we use instead of Eq. (1) for simplicity

$$\sigma_{ij} = (1 - Q) \times \sigma_{ij}^h + Q \times \sigma_{ij}^e, \quad Q = \frac{a + b|H/S^t|}{1 + |H/S^t|}, \quad (3)$$

where  $Q$  is a weighting factor and  $a$  as well as  $b$  are the relative contributions of the electron conductivity at zero and high fields, respectively.  $S^t$  is proportional to the scattering rate for the transition from holelike to electronlike orbits. Although this model is very simple, we are able to model both  $\rho_{xx}(H)$  and  $\rho_{xy}(H)$  for all our four samples in the temperature interval, where the ordinary Hall effect is dominant. For the lowest temperature, we indicate the fits as open circles in Fig. 1. The corresponding parameters are listed in Table I, the densities  $n \times Q$  and (only for *S1*)  $p \times (1 - Q)$  are shown in Fig. 3 as a function of the magnetic field.

The main result of this model is that the low-temperature carrier transport is dominated by holes at zero magnetic field in  $A_0$ -oriented MnAs films. Electrons appear at the expense of holes with increasing magnetic field. In contrast, samples with an out-of-plane orientation of the MnAs  $c$  axis exhibit mixed holelike and electronlike conductivity already at zero magnetic field. The conductivity in sample *S4* even shows the signature of a compensated metal with nearly equal hole and electron density. Because of the simplicity of the model and the arbitrarily chosen weighting factor  $Q$ , the densities and inverse mobilities given in Table I are more an estimation rather than a precise determination. At least, the estimated mean free path  $L^h$  from these values are of the order of the film thickness, which indicates that scattering occurs mainly at the surface and at the MnAs/GaAs interface as expected for the low-temperature case. Both the inverse mo-

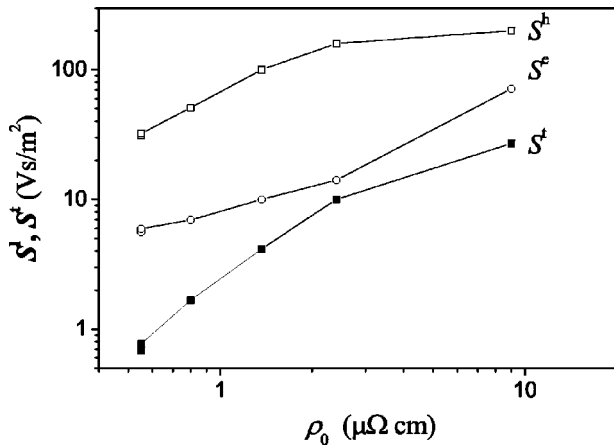


FIG. 4. Dependence of  $S^h$ ,  $S^e$ , and  $S^t$  on the zero-field resistivity for samples S1 ( $\rho_0 \leq 3 \mu\Omega$  cm) and S2 ( $\rho_0 = 9 \mu\Omega$  cm).

bilities as well as  $S^t$  increase with increasing film resistivity, as shown in Fig. 4. The absolute values of  $S^t$  are always lower than  $S^h$  and  $S^e$ . At the same time, the condition  $\omega_c \tau = H/S^t > 1$ , for which carriers may complete full circles around orbits at the Fermi surface, is not fulfilled for both holes and electrons in our experiment. Instead, the condition  $H/S^t > 1$  seems to control the sign reversal of the Hall resistivity and is responsible for the universality of the data in the Kohler plot shown in Fig. 2. We do not fully understand the reason for this discrepancy. However, a possible basis for an explanation may be the dominance of surface and interface scattering, which are characterized by specular and diffuse scattering processes. A strong diffuse scattering at the interface/surface redistributes carriers over a wide area of momentum space at the Fermi surface, thus increasing both  $S^l$  and  $S^t$  (see Fig. 4). During the motion across the film from

the surface to the interface and back, the carriers cannot accumulate sufficient wave-vector change from the magnetic flux in order to reach other regions at the Fermi surface, which have a different curvature. In contrast, specular scattering changes only the momentum projection perpendicular to the surface or interface, leaving the momentum in the film plane unchanged. High-resolution transmission electron microscopy reveals an abrupt interface between the MnAs layer and GaAs(001).<sup>18</sup> Therefore, we suppose that specular scattering exists in our films, which enables a low number of carriers to remain longer in orbits around the Fermi surface, thus to accumulate sufficient wave-vector change to reach electronlike orbits. Path-integral calculations including interface scattering are necessary to check whether such processes can explain the present experimental results.

In conclusion, the carrier type for transport in thin MnAs layers on GaAs depends sensitively on the crystal orientation and the magnetic field. We used a simplified model to interpret the results of low-temperature magnetoresistance measurements, which indicate a change of the carrier type with increasing magnetic field. As a result, we found for  $A_0$ -oriented MnAs films that the low-temperature carrier transport is dominated by holes at zero magnetic fields with a transition to electronlike conductivity at high magnetic fields. We speculate that a possible specular scattering at the interfaces increases the lifetime of carriers on momentum orbits at the Fermi surface making the transition possible. MnAs films with an out-of-plane component of the c-axis show a mixed carrier conductivity already at zero magnetic fields.

The authors would like to thank C. Herrmann and A. Riedel for technical assistance. We are indebted to K. H. Ploog for continuous support and to H. T. Grahn for a critical reading of the manuscript.

\*Electronic address: kjf@pdi-berlin.de

<sup>1</sup>H. J. Zhu, M. Ramsteiner, H. Kostial, M. Wassermeier, H. P. Schönherr, and K. H. Ploog, Phys. Rev. Lett. **87**, 016601 (2001).

<sup>2</sup>A. T. Hanbicki, B. T. Jonker, G. Itkos, G. Kioseoglou, and A. Petrou, Appl. Phys. Lett. **80**, 1240 (2002).

<sup>3</sup>M. Tanaka, J. P. Harbison, M. C. Park, Y. S. Park, T. Shin, and G. M. Rothberg, J. Appl. Phys. **76**, 6278 (1994).

<sup>4</sup>L. Däweritz, F. Schippan, A. Trampert, M. Kästner, G. Behme, Z. M. Wang, M. Moreno, P. Schützendübe, and K. H. Ploog, J. Cryst. Growth **227-228**, 834 (2001), and references therein.

<sup>5</sup>J. J. Berry, S. J. Potashnik, S. H. Chun, K. C. Ku, P. Schiffer, and N. Samarth, Phys. Rev. B **64**, 052408 (2001).

<sup>6</sup>C. M. Hurd, J. E. A. Alderson, and S. P. McAlister, Phys. Rev. B **14**, 395 (1976).

<sup>7</sup>R. V. Coleman, R. W. Klaffky, and W. H. Lowrey, in *The Hall Effect and its Applications*, edited by C. L. Chien and C. R. Westgate (Plenum, New York, 1980), p. 99.

<sup>8</sup>Concerning the GaAs(001)- $d(4 \times 4)$  surface structure, see, e.g., I. Kamiya, D. E. Aspnes, L. T. Florez, and J. P. Harbison, Phys. Rev. B **46**, 15 894 (1992).

<sup>9</sup>F. Schippan, G. Behme, L. Däweritz, K. H. Ploog, B. Dennis, K.-U. Neumann, and K. R. A. Ziebeck, J. Appl. Phys. **88**, 2766 (2000).

<sup>10</sup>Y. Morishita, K. Ida, J. Abe, and K. Sato, Jpn. J. Appl. Phys., Part 2 **36**, L1100 (1997).

<sup>11</sup>S. M. Watts, S. Wirth, S. von Molnar, A. Barry, and J. M. D. Coey, Phys. Rev. B **61**, 9621 (2000).

<sup>12</sup>L. Berger, Phys. Rev. **177**, 790 (1969).

<sup>13</sup>N. W. Ashcroft and N. D. Mermin, in *Solid State Physics* (Holt, Rinehart, and Winston, New York, 1976), Chap. 12.

<sup>14</sup>C. M. Hurd, in *The Hall Effect and its Applications*, edited by C. L. Chien and C. R. Westgate (Plenum, New York, 1980), p. 1.

<sup>15</sup>L. M. Sandratskii, R. F. Egorov, and A. A. Berdyshev, Phys. Status Solidi B **103**, 511 (1981).

<sup>16</sup>P. Ravindran, A. Delin, P. James, B. Johansson, J. M. Wills, R. Ahuja, and O. Eriksson, Phys. Rev. B **59**, 15 680 (1999).

<sup>17</sup>S. Sanvito and N. A. Hill, Phys. Rev. B **62**, 15 553 (2000).

<sup>18</sup>F. Schippan, A. Trampert, L. Däweritz, and K. H. Ploog, J. Vac. Sci. Technol. B **17**, 1716 (1999).